

The Effect of Debonding on the Flexural Behaviour of Reinforced Concrete Beams Strengthened with Fibre Reinforced Polymer

Warna (Karu) Karunasena¹ and Nicole Martin²

¹*Faculty of Engineering and Surveying, University of Southern Queensland, Toowoomba, Qld 4350*
Email: Karu.Karunasena@usq.edu.au

²*Sinclair Knight Merz, 2 James St, Cairns, Qld 4870*

Abstract: In recent years, the use of fibre reinforced polymer (FRP) as a means of rehabilitating or strengthening reinforced concrete (RC) beams has generated much interest in the construction industry. The most popular means of utilising FRP for this purpose involves externally bonding the FRP strip to the extreme tensile fibres of the beam. In previous work, predictions on the behaviour of a beam undergoing debonding have been made utilising experimental FRP strain data to account for the strain incompatibility at the debonded zone. In this paper, previous work has been extended such that strain incompatibility is taken into account through a simple theoretical development to the simple beam theory rather than using experimental measurements of FRP strain data. The model has been verified and used to study the effect of debond length on the flexural behaviour of the beam.

Keywords: debonding, fibre reinforced polymer, flexural behaviour, load-deflection relation, moment-curvature relation, reinforced concrete beams.

1 Introduction

The need for an efficient means of rehabilitating and upgrading existing concrete structures has become increasingly apparent in recent years. Corroded steel reinforcement, flaws in the original construction of the beam or damage from impact or environmental conditions are common reasons that a structure may require rehabilitation. Upgrading the structure by strengthening its main structural elements may also be important, due to a change in the use of structure, and hence different loading conditions than were originally designed for. Conventional techniques of rehabilitating or strengthening RC beams in bridges and other significant structures are usually costly, time consuming and not always efficient. For these reasons, the recent development of retrofitting RC beams with FRP is attracting much attention from the construction industry and the researchers alike.

The general properties of FRP make it ideal for rehabilitation. Being resistant to electrochemical corrosion and having a high strength to weight ratio are two properties that set this material apart from steel. These properties aid in easy installation and therefore there is minimal disruption to the use of the structure. Although FRP is more costly than steel, the money that is saved through time and low installation costs still makes FRP a favourable option for rehabilitation and strengthening existing concrete beams, specially when life cycle costs are taken into account.

The oldest and currently most prominent technique available to utilise FRP in this application involves externally bonding FRP laminate to the extreme tensile side of the RC beam. A RC beam retrofitted with FRP in this way can fail through a number of ways, depending on how the FRP was fitted. Failures can be categorised into two types – sectional failure and debond failure ([1], [2]). Failure through debonding is still not fully understood, although several models have been developed with reasonable success. The FRP is known to debond at the intermediate span, as well as at the end of the externally bonded strip. To add to this, debonding is the most common mode of failure for RC beams fitted with FRP.

The primary objective of this study was to further understand the behaviour of a RC beam fitted with FRP and undergoing debonding at the mid-span. This was achieved through applying a sectional analysis to develop a fully analytical model to predict the moment-curvature and load-deflection behaviour of such a beam. The results of this model are verified using experimental data from the literature. Finally, a parametric analysis is undertaken using the model to find the effects of varying debonded lengths of FRP, and different concrete characteristic compressive strengths, on the behaviour of the beam.

2 Prediction Model

The model that will be used to compute the moment-curvature relations is based on the assumed stress-strain distributions for concrete, steel and FRP in the beam. This type of analysis has been presented before by Ross et al. [3], however no debonding effects were taken into account in their analysis. The model was later modified by Chahrour and Soudki [4] who adapted the model to predict the moment-curvature relationships for beams with varying debonded lengths of CFRP, by using measured stains data, to account for the strain incompatibility between FRP and concrete in the debonded section.

A linear stress-strain relationship has been assumed for the concrete, and the steel stress-strain relationship does not account for strain hardening. The assumed stress-strain relationships are shown in Figure 1. From these simplified stress-strain relationships, three zones are assumed for the moment-curvature relationship, which is shown in Figure 1 (d).

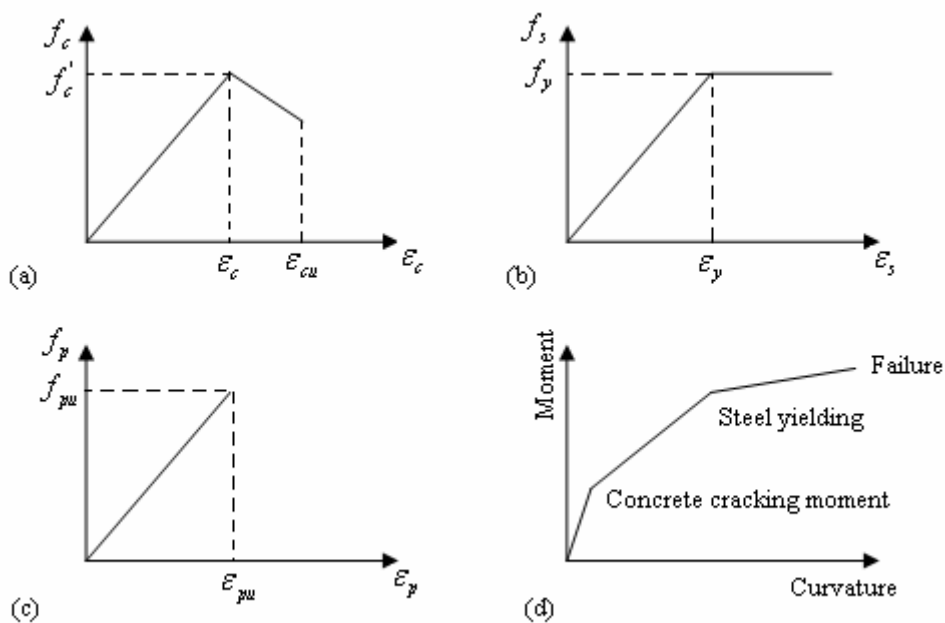


Figure 1: Assumed deformation models: (a) concrete stress-strain model; (b) steel stress-strain model; (c) FRP stress-strain model; (d) moment-curvature response

2.1 Sectional Analysis

The model is based on a sectional analysis of the beam at three different behavioural zones. In the first zone, the beam is analysed as an uncracked section. This zone is terminated at the concrete cracking moment. Zone 2 is analysed as a cracked section, with this zone terminating when the tensile steel in the beam yields. Finally, zone 3 is analysed as a cracked section with yielded tensile steel. For the purpose of the model presented in this paper, the termination point of zone 3, or the failure point of the beam, is assumed to occur at the characteristic compressive strength of the concrete.

Figure 2 shows the stress and strain distributions that the analysis is based on, for each of the three zones. To establish a fully analytical model, a relationship between the strain in the debonded FRP and the strain in the compressive fibres of the concrete need to be developed. In order to do this, the primary assumption, of which all predictions have been based on, is that the debonded length of FRP acts as a tension member. By making this assumption, the strain in the FRP at the end of the debonded zone can be found by applying strain compatibility. This FRP strain can then be assumed constant for the whole debonded length of FRP as a tension member has same tensile strain (and tensile stress) at any location over its length.

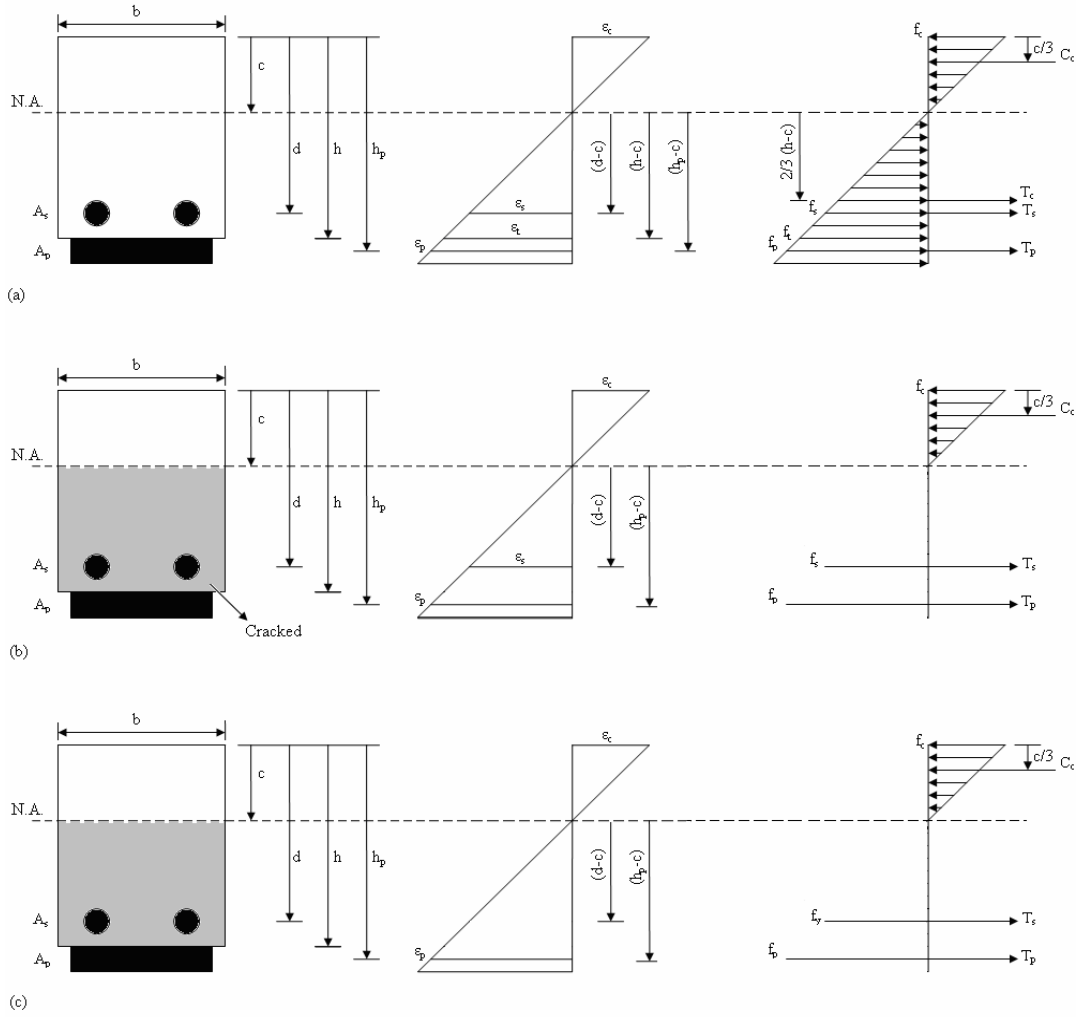


Figure 2: Assumed strain and stress distributions:
 (a) complete elastic behaviour – zone 1; (b) concrete cracked in tension zone – zone 2;
 (c) concrete cracked in tension zone, tensile steel yielded – zone 3

Firstly, the moment-curvature relationship for beam when FRP is fully bonded is established. With reference to Figure 2, the equilibrium of forces in each of the zones results in:

$$\sum F = 0 \Rightarrow C_c - T_c - T_s - T_p = 0 \quad (1)$$

where resultant compressive force of the concrete (C_c), the resultant tensile force of the concrete (T_c), the tensile force of the steel (T_s) and the tensile force of the CFRP (T_p) are as labelled in Figure 2. Using strain compatibility, stress-strain relations and the stress distribution blocks given in Figure 2, simple expressions for C_c , T_c , T_s and T_p can be derived in terms of known material properties, geometric dimensions and the unknown neutral axis depth c . Substitution of these expressions in (1) result in the following equations to solve for c for no debonding situation [3] :

$$\text{Zone 1} \rightarrow c = \frac{h^2 + 2N_s A_s \frac{d}{b} + 2N_p \frac{A_p}{b} h}{2h + 2N_s \frac{A_s}{b} + 2N_p \frac{A_p}{b}} \quad (2)$$

$$\text{Zone 2} \rightarrow c^2 + 2 \left(\frac{A_s N_s}{b} + \frac{A_p N_p}{b} \right) c - 2 \left(\frac{A_p N_p h}{b} + \frac{A_s N_s d}{b} \right) = 0 \quad (3)$$

$$\text{Zone 3} \rightarrow e_c E_c b c^2 - (2A_s f_y - 2A_p E_p e_c) c - 2A_p E_p e_c h = 0 \quad (4)$$

where the dimensions h , d , b are as defined in Figure 2, and A_s is the area of steel, A_p is the area of FRP, and E_c , E_s , and E_p , are Young's modulus of elasticity of concrete, steel and FRP, respectively. N_s and N_p are equal to E_s/E_c and E_p/E_c , respectively, and ϵ_c is the strain in the extreme compressive concrete fibres.

After determining c from equations (2) to (4) for different zones, section moment M can be determined by taking moments about the centroidal axis of the section. The curvature of the beam is given by

$$f = \frac{e_c}{c} . \quad (5)$$

Now by increasing ϵ_c from 0 to ϵ_c' ($=f_c'/E_c$), points on the moment-curvature relation plot for no debonding case can be determined.

To extend the model from here to accommodate for a beam with a debonded length of FRP at the mid-span, a relationship between the strain in the debonded FRP (ϵ_p) and ϵ_c is required. The approach here is to determine the strain in the debonded length of FRP using the moment-curvature relationship for no debonding case. In this approach, for a given loading condition, the moment at the section where debonding ends (M_1) is determined first. At this section, FRP is bonded to concrete on one side (left or right) and debonded on the other side (right or left). It is also assumed that the FRP strain at the immediate vicinity of the left and right sides of this section are same. Using the moment-curvature relationship for no debonding case, the curvature corresponding to M_1 can be determined. The depth of the neutral axis (c) for the appropriate zone can be determined from (2) to (4). Now, ϵ_c can be computed using (5). Hence, the strain in the FRP can be determined using strain distribution diagrams in Figure 2 as

$$e_p = e_c \frac{(h_p - c)}{c} . \quad (6)$$

Using our main assumption that debonded segment of the FRP acts as a tension member, FRP strain calculated from (6) is assumed to be constant for the whole debonded length. With the FRP strain known, moment and curvature at any section can be computed following the above formulation. Thus moment-curvature relation for the debonded FRP beam can be generated.

2.2 Load-Deflection Relation

The moment-curvature relationship for a beam undergoing a given length of debonding is a vital step in finding the load-deflection behaviour for the given beam. In this case, the load-deflection behaviour is predicted for the mid-span of the beam, as this is usually where the maximum deflection occurs.

The virtual work principle is applied to calculate the deflections in the beam. The virtual work method calculates deflections, given the curvature distribution along the length (L) of the beam, thus making this principle valid for linear and nonlinear stress range deflections, unlike other available techniques. Expressed mathematically:

$$d = \int_{x=0}^{x=L} f(x) . m_v(x) . dx \quad (7)$$

where d is mid-span deflection, $f(x)$ is the curvature distribution along the length of the beam, x , and $m_v(x)$ is the moment distribution along the length of the beam which has resulted from a virtual unit load being placed on the beam (in this case at the mid-span). Four-point and three-point bending will be used as the loading scenarios for the purpose of this paper. As the method is formulated to take into account a given debond length at the mid-span, the strain along the beam will be dependant on the whether the FRP is bonded or debonded at a given section. This, in turn, will affect the curvature distribution along the beam. For this reason numerical integration need to be used to evaluate deflection d in (7). For a given loading condition, the curvature distribution can be determined as described in the previous section 2.1. Thereafter, the Simpson's rule was used to numerically evaluate d for a given load. In the next section, results for the deflection are presented in the form of load-deflection relations.

3 Numerical Results and Discussion

Numerical analysis was carried out on a beam with the characteristics of that used in Chahrour and Soudki [4] so that present model results can be verified using the experimental results obtained from their analysis. Unless otherwise specified, the dimensions of the beam and the material properties are: $L = 2250$ mm, $b = 150$ mm, $h = 250$ mm, $d = 219$ mm, $A_s = 353$ mm², and $A_p = 120$ mm²; Young's modulus of the steel, concrete and FRP are 200 GPa, 28.1 GPa and 155 GPa, respectively; $f'_c = 39$ MPa; and the yield stress f_y of steel is 400 MPa.

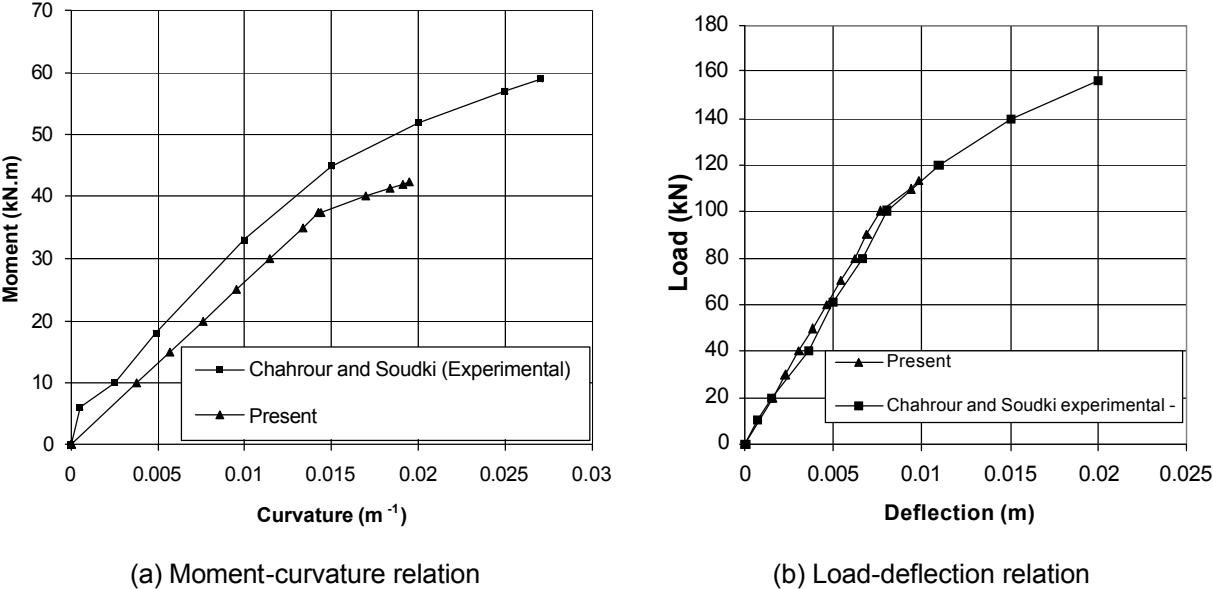


Figure 3: Flexural behaviour of a beam with a 250 mm FRP debond length at the mid-span, loaded under four point bending.

A comparison of flexural behaviour prediction from the present model with the experimental results presented in [4] is shown in Figure 3. Model predictions show reasonable agreement with the experimental results. Any differences in results could be due to the facts that the non-linear concrete behaviour has been simplified as linear and the strain-hardening effect of steel has been ignored.

The model was used to investigate the effect of varying lengths of debonding on the behaviour of the beam subjected to four point bending with load points at one-third and two-third of span. Load-deflection results for 0 mm, 1000 mm and 1250 mm debond lengths are presented in Figure 4. It is evident from this figure that beams with a higher length of debonding have a lower failure load. Figure 5 shows the effects of varying lengths of debonding, as well as an increased characteristic compressive strength, on the behaviour of the beam under three point bending loading condition. It

can be seen from this figure that for three-point loading, small debond lengths have significant effect on the strength of the beam. The figure also shows that when the characteristic compressive strength of the beam is increased, the effects of these small lengths of debonding are amplified. Also it can be seen from both Figures 4 and 5 that FRP has only a very small influence on the load-deflection plots before the tensile steel yields. FRP starts taking significant loads only after steel yields.

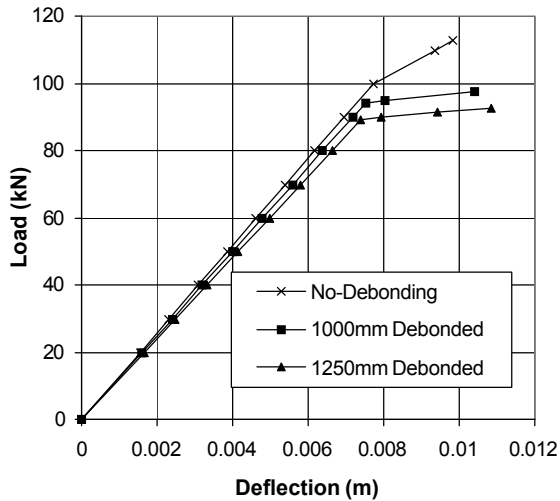


Figure 4: Influence of the debond length on the load-deflection behaviour under four point bending loading.

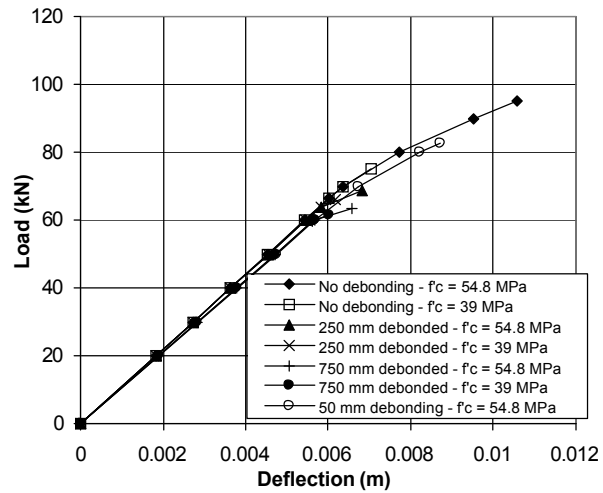


Figure 5: Influence of the debond length and concrete strength on the load-deflection behaviour under three bending loading.

4 Conclusions

A simple model that can predict the flexural behaviour of a FRP reinforced RC beam with some debonding of the FRP near the mid-span of the beam has been developed, and the model verified by comparison with experimental behaviour. A parametric analysis has shown that the smaller the debonded length, the higher the load capacity of the beam. Analysis has also shown that contribution of FRP becomes significant only after tensile steel yields. Furthermore, it was found that, as the concrete strength increases, the length of the debonding has an increasing effect on the strength of the beam. The current model has its limitations as it does not take into account the non-linear concrete behaviour and the strain hardening effects of steel. Nevertheless, the developed model can be used to make preliminary predictions on the flexural behaviour of debonded FRP beams.

4 References

- [1] Pham, H. B., and Al-Mahaidi, R. (2006). "Prediction Models for Debonding Failure Loads of Carbon Fiber Reinforced Polymer Retrofitted Reinforced Concrete Beams." *Journal of Composites for Construction*, 10(1), 48-59.
- [2] Thomsen, H., Spacone, E., Limkatanyu, S., and Camata, G. (2004). "Failure Mode Analyses of Reinforced Concrete Beams Strengthened in Flexure with Externally Bonded Fiber-Reinforced Polymers." *Journal of Composites for Construction*, 8(2), 123-131.
- [3] Ross, C. A., Jerome, D. M., Tedesco, J. W., and Hughes, M. L. (1999). "Strengthening of Reinforced Concrete Beams with Externally Bonded Composite Laminates." *Aci Structural Journal*, 96(2), 212-220.
- [4] Chahrouh, A., and Soudki, K. (2005). "Flexural Response of Reinforced Concrete Beams Strengthened with End-Anchored Partially Bonded Carbon Fiber-Reinforced Polymer Strips." *Journal of Composites for Construction*, 9(2), 170-177.